



# Mathematical theories for two classes of thermoelastic contact problems

Peter Howell<sup>a</sup>, John Ockendon<sup>a,\*</sup>, Meir Shillor<sup>b</sup>

<sup>a</sup> OCIAM, Mathematical Institute, Andrew Wiles Building, Oxford OX2 6GG, UK

<sup>b</sup> Department of Mathematics and Statistics, Oakland University, Rochester, MI 48309-4401, USA

## ARTICLE INFO

### Keywords:

Contact conditions

Wear

Mathematical analysis

Asymptotic analysis

## ABSTRACT

This paper reviews some of the mathematical research that has been inspired by Jim Barber's pioneering experimental and theoretical work on thermoelastic contact problems. The first part considers rod-contact problems in the absence of wear, but allowing for elastic waves, and the second part focuses on the effect of wear over time-scales when elastic waves are negligible.

## 1. Introduction

It is unusual for mathematicians to contribute theoretical articles to journals in materials and engineering science. However, when the article is part of a tribute to Jim Barber, we have the opportunity to describe some of his original ideas from the mathematical point of view. Few of Jim's papers have been published in mathematical journals, and we hope that what follows will encourage mutually beneficial collaborations of the kind we have had with Jim.

Most of Jim's papers contain some mathematics, and this is certainly true in the area of thermoelastic contact which will be the focus of this paper. To review all Jim's contributions in this area would be a lengthy task and we will only concentrate on two themes; namely, the modelling of multi-pin contact problems of the type pioneered in Barber (1969), and the formulation of thermal boundary conditions and their applications in more general thermoelastic contact problems, as pioneered in Barber (1978).

The question of posing realistic boundary conditions in such thermoelastic contact problems is the basis for the mathematical challenge discussed in Section 2. In Barber (1978), the usual heat transfer boundary condition was replaced by a temperature condition when there is perfect contact, an insulation condition when there is no contact, and an 'imperfect' thermal condition when there is contact with zero stress. The consequent coupling of this boundary condition with the usual assumptions of stress continuity and non-interpenetration has been much studied in recent years, much of the research having been motivated by the modelling of micro-electrical-mechanical-systems (MEMS) devices, such as actuators, grippers and other micro-devices that populate our cell phones, computers and almost all things electronic. Such processes appear also in many other applications that involve frictional heat generation, such as in braking systems, where considerable amounts

of energy are released, and in the contact of wheels with a road or railway.

The research in Barber (1969) was motivated by the need to quantify phenomena such as the sliding of brake blocks. However, even today, this research is not well-known in the mathematical community. Indeed, we were unaware of the paper until we heard Jim give a seminar 10 years ago. The proposed theory was quite different from the conventional stick/slip models for spragging that were prevalent at the time. Basically it relied on the repeated volumetric growth and decay of hot spots at the ends of elastic pins pressed against a moving substrate. The calculations in Barber (1969) were constrained by the limitations of contemporary computers, but a novel dynamical system was proposed describing heat transfer in rods whose lengths change in response to frictional heating and wear at one end, where a simple heat transfer condition was applied. The model showed that, for just one pin, wear always prevails and contact is eventually lost. For two pins, however, wear was found to be able to transfer from one to the other repeatedly, with simultaneous contact only occurring over short time intervals.

Thermoelastic contact problem come under the mathematical heading of 'free boundary problems' and, for problems involving change of phase, the theory is often simplified by introducing enthalpy, combining sensible and latent heat, as a dependent variable. It is interesting that an enthalpy-like variable also plays a key role in the posing of Barber's 'imperfect' thermal condition, this time involving a combination of thermoelastic displacement and stress. The introduction of the 'imperfect' thermal contact condition in Barber (1978) came right at the time when the mathematical theory of variational methods and the associated weak solutions was under intensive development. The condition, termed the 'Barber's heat exchange condition' when recast

\* Corresponding author.

E-mail address: [ock@maths.ox.ac.uk](mailto:ock@maths.ox.ac.uk) (J. Ockendon).

in the language of variational inequalities in Andrews et al. (1993), was of the type that the emerging theory was ready to address and be incorporated into the Mathematical Theory of Contact Mechanics (MTCM). The Barber condition not only fits well within the theory of variational inequalities and differential set-inclusions, but it also serves as an impetus for the further development and extension of MTCM.

The relevant mathematical literature mostly deals with the modelling and analysis of various settings in which dynamic or quasistatic contact is accompanied by thermal effects, but computer simulations using this condition are rarely validated mathematically. This is despite the fact that variational formulations of such models translate directly into Finite Elements algorithms. But, the condition is non-smooth and must be regularised both for analysis and computational reasons.

Below, in Section 2, we introduce the relevant concepts of variational inequalities and differential inclusions in the relatively simple setting of one-dimensional purely elastic contact. We then derive a simple model for one-dimensional contact of a single thermoelastic rod, which is then used to motivate the posing of Barber's heat exchange condition. We also show a recent application of the condition to a MEMS actuator.

In Section 3 we show how wear can be incorporated into the one-dimensional thermoelastic contact problem formulated in Section 2, before generalising the setup to model Barber's original 1969 experiment (Barber, 1969) with, in principle, an arbitrary number  $N$  of pins. We again find that the mathematical formulation hinges on the use of an enthalpy-like contact variable, which satisfies a novel non-local and non-smooth evolution equation. We demonstrate the surprisingly rich dynamics of the resulting system in the particular cases  $N = 2$  and  $N = 3$ .

## 2. Barber's thermal boundary conditions

### 2.1. Background

This section deals with the mathematical aspects and applications of the so-called 'Barber's heat exchange condition', which describes the thermal interaction upon contact between a thermoelastic body and a rigid thermally active foundation, in the absence of wear. The introduction of this condition into contact models in the late 90's and early 20th century (see Andrews et al., 1993; Xu, 1996; Shillor et al., 2004; Sofonea et al., 2006; Shillor, 2013 and the many references therein) resulted in the expansion of the Mathematical Theory of Contact Mechanics (MTCM) to include thermal effects. Currently, there are some mathematical publications at various levels of abstraction and applications (see Ahn et al., 2017; Bartosz et al., 2018; Bień, 2003; Gasiński et al., 2016; Migórski et al., 2018; Shillor, 2020 and the many references therein). As was noted in the Introduction, the number of applications of the MTCM to MEMS is increasing and the models and mathematical problems are becoming more sophisticated, especially those that deal with the combined processes of thermoelastic contact and Joule heating. Such settings abound in MEMS, and below in Section 2.5, we describe such a setting in some detail.

### 2.2. Contact conditions

To describe the condition in the current mathematical setting, we first model the so-called 'Signorini non-penetration contact condition', for the process of contact between a body and a perfectly rigid object, which typically is called 'foundation'. Then, we add thermal effects and introduce Barber's heat exchange condition.

We initially use a zero-dimensional and then a one-dimensional setting for the description of contact conditions. This avoids the introduction of various mathematical notation related to the contacting surfaces. First, we present the Signorini contact condition for a spring-mass system (ODE), then, we add thermal effects in the model for a thin rod. We consider the usual mass-spring model, Fig. 1, where the

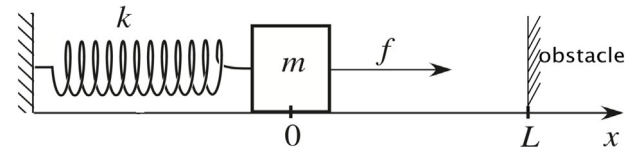


Fig. 1. The setting of the mass-spring system; the perfectly rigid obstacle is positioned at  $x = L$ .

body is vibrating horizontally on a surface, or a rail, that does not resist the motion, the so-called 'frictionless' case. However, the motion is constrained as the mass may come into contact with an obstacle situated at  $x = L$ , in the absence of wear. We use *contact* to indicate either a gentle (continuous) contact, or an *impact*, which describes an abrupt or impulsive (discontinuous velocity) contact.

As long as the body does not come into contact with the obstacle, the vibrations are those of the usual linear spring-mass system. However, here our interest is in the contact process. In the MTCM literature this is described either by the *Signorini contact condition*, which assumes that the obstacle is perfectly rigid, or by the *normal compliance condition*, which assumes that the obstacle is reactive, or a combination of the two. Here, our interest is in the former.<sup>1</sup>

Since we assume that the obstacle is perfectly rigid, the displacement  $x(t)$  (from the equilibrium point  $x = 0$ ) must satisfy

$$x(t) \leq L, \quad (2.1)$$

which explains why it is also called the *nonpenetration condition* or *unilateral condition*. Then, when there is contact,  $x = L$  and the force exerted by the obstacle  $F_{Sig}$  prevents the body from exceeding  $x = L$ .

We may write the equation of motion as

$$x'' + kx = f + F_{Sig}. \quad (2.2)$$

The difficulty with this expression is that there is no 'simple' way to find  $F_{Sig}$ . Actually, it may not be a traditional function, but a distribution (such as the 'Dirac delta function'), acting only at the instants of contact. To bring it into a form that allows us to use the tools of the modern analysis, we recast the problem as an inequality. Indeed, we know that  $F_{Sig} \leq 0$ , since the reaction acts to the left, so

$$x'' + kx - f \leq 0.$$

This leads to the following *complementarity conditions*:

$$x \leq L, \quad x'' + kx - f \leq 0, \quad (x'' + kx - f)(x - L) = 0. \quad (2.3)$$

The last condition guarantees that the two inequalities cannot be strict at the same time, since either there is contact and  $x = L$ , or there is no contact and  $F_{Sig} = 0$ , and then  $x'' + kx - f = 0$ . In addition, we prescribe two initial conditions  $x(0) = x_0 \leq L$  and  $x'(0) = v_0$ . More details can be found in Shillor et al. (2004) and the many references therein.

Next, we recast the problem as a variational inequality. To that end, let  $V$  be the vector space of test functions  $\psi$  for the problem,<sup>2</sup> defined on  $[0, T]$ , such that  $\psi(t) \leq L$ , for  $0 \leq t \leq T$  and  $\psi(0) = x_0$ . We multiply (2.2) by  $\psi - x$ , where  $\psi \in V$ , integrate over  $[0, T]$ , and notice from (2.3) that  $(L - x(t))F_{Sig}(t) = 0$  and  $(\psi(t) - L)F_{Sig}(t) \geq 0$ , and hence

$$\int_0^T (\psi(t) - x(t))F_{Sig}(t) dt = \int_0^T (\psi(t) - L + L - x(t))F_{Sig}(t) dt \geq 0.$$

<sup>1</sup> See, e.g., Fichera (1972), and also Duvaut and Lions (1976), Kikuchi and Oden (1988). We note that in the MTCM literature it is often claimed that Signorini formulated the condition as a 'vague condition', and his student Fichera introduced the term 'The Signorini contact condition'.

<sup>2</sup> All measurable functions with measurable and integrable first weak derivatives.

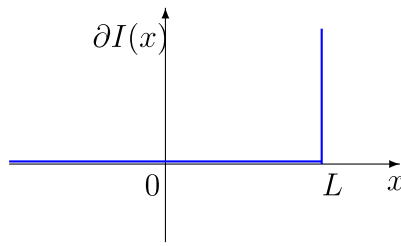


Fig. 2. The graph  $\partial I(x)$  (blue).

Since the velocity  $x'$  may be discontinuous, we use integration by parts to transfer one derivative to the test function, thus allowing us to seek the solution  $x$  in the space  $V$ . Thus, using the fact that  $\psi(0) = x(0) = x_0$ , we find

$$\int_0^T x''(\psi(t) - x(t)) dt = - \int_0^T x'(\psi(t) - x(t))' dt + x'(T)(\psi(T) - x(T)).$$

Thus, by dropping a nonnegative term on the right-hand side we obtain the *variational inequality formulation of the problem*:

Find  $x \in V$  such that for each  $\psi \in V$ ,

$$\begin{aligned} & - \int_0^T x'(\psi'(t) - x'(t)) dt + x'(T)(\psi(T) - x(T)) \\ & + \int_0^T (kx(t) - f(t))(\psi(t) - x(t)) dt \geq 0. \end{aligned} \quad (2.4)$$

Finally, we note that we can set the problem in an equivalent form as a set-inclusion, which is another way to describe the Signorini condition. To that end, we consider the set-valued function or graph  $\partial I$ , the so-called ‘subdifferential’ of the indicator function of the set  $(-\infty, L]$ , defined as

$$\partial I(x) = \begin{cases} 0 & -\infty < x < L, \\ [0, \infty) & x = L. \end{cases} \quad (2.5)$$

The graph  $\partial I(x)$  is depicted in Fig. 2. Then, the Signorini condition means that  $-F_{Sig}(t) \in \partial I(x(t))$ , for  $0 \leq t \leq T$ . Indeed,  $F_{Sig}(t) = 0$  when  $x(t) < L$  and  $F_{Sig}(t)$  has a negative value when  $x(t) = L$ . Therefore, we may rewrite the problem in an equivalent form as a *differential inclusion*: Find  $x \in V$  such that,

$$x'' + kx - f \in -\partial I(x), \quad a.e. (0, T). \quad (2.6)$$

In addition, we require that  $x(0) = x_0$ ,  $x'(0) = v_0$ .<sup>3</sup>

It can be shown that the three forms of the problem are equivalent and when  $x_0 \leq L$  and that when the applied force  $f$  is continuous, the problem has a unique weak solution  $x \in V$ .

### 2.3. Thermal contact conditions

When we consider the thermal aspects in contact mechanics, the simplest configuration is that of a thermoelastic rod. We consider the simple setting depicted in Fig. 3 of a thermoelastic rod that occupies the interval  $0 \leq x \leq L$ . Let  $u = u(x, t)$  represent the horizontal displacement of the point  $x$  at time  $t$ , and let  $\theta(x, t)$  represent the absolute temperature. Then, following Carlson (1973), the energy equation is

$$\rho c \theta_t - k \theta_{xx} = -\theta_0 \alpha (3\lambda + 2\mu) u_{xt},$$

and the dynamic equation for the displacement is

$$\rho u_{tt} - (\lambda + 2\mu) u_{xx} = -\alpha (3\lambda + 2\mu) \theta_x.$$

Here the subscripts  $x, t$  denote partial derivatives,  $\rho$  is the material density,  $c$  the heat capacity,  $k$  the coefficient of thermal conductivity,

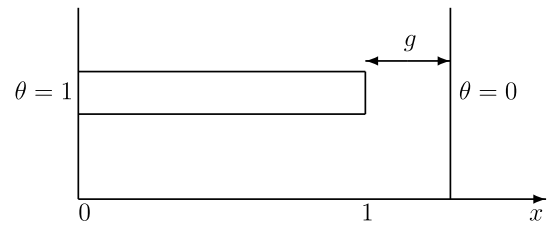


Fig. 3. The physical setting: a thermoelastic rod separated from an obstacle by a gap  $g$ .

$\lambda$  and  $\mu$  the Lamé coefficients,  $\alpha$  the coefficient of thermal expansion and  $\theta_0$  is a reference or ambient temperature, all positive constants. We rescale the problem from the original interval  $[0, L]$  to the unit interval  $[0, 1]$ , and set the system in a dimensionless form. Let us denote a typical temperature variation across the rod by  $\Delta\theta$ . The change of variables

$$x \rightarrow \frac{x}{L}, \quad t \rightarrow \frac{kt}{\rho c L^2}, \quad \theta \rightarrow \frac{\theta - \theta_0}{\Delta\theta} \quad \text{and} \quad u \rightarrow \frac{u}{L} \frac{\lambda + 2\mu}{(3\lambda + 2\mu)\alpha \Delta\theta}, \quad (2.7)$$

transforms the equations into

$$\theta_t - \theta_{xx} = -a^2 u_{xt} \quad (2.8a)$$

$$b u_{tt} - u_{xx} = -\theta_x, \quad (2.8b)$$

respectively; here, the *coupling constant*  $a$  and the *inertial constant*  $b$  are given by

$$a^2 = \frac{\theta_0 \alpha^2 (3\lambda + 2\mu)^2}{\rho c (\lambda + 2\mu)}, \quad b = \frac{k^2}{\rho c^2 (\lambda + 2\mu) L^2}, \quad (2.9)$$

and the dimensionless stress in the rod  $\sigma = \sigma(x, t)$  is given by

$$\sigma = u_x - \theta. \quad (2.10)$$

It turns out that in many applications  $a$ , which is proportional to the coefficient of thermal expansion, is small and  $b$  is very small. When it is reasonable to expect small accelerations in the process, the term  $b u_{tt}$  is likely to be negligible, and the resulting system, obtained by setting  $b = 0$ , is called *quasistatic*.

The setting is depicted in Fig. 3, where the rod is attached to a wall at  $x = 0$  and may come in contact with a rigid obstacle situated at  $x = 1 + g$ , so that  $g \geq 0$  is the gap (in reference configuration). The obstacle is kept at zero temperature. To complete the model we have to take into account initial and boundary conditions. Since our main interest lies in the contact conditions, we choose simple boundary conditions at the left edge, namely that the rod is held fixed,  $u = 0$ , and maintained at constant temperature, say  $\theta = 1$ .

We also need the contact and thermal conditions at the free edge  $x = 1$ . The displacement boundary condition is the Signorini condition, which in this setting reads,

$$u \leq g, \quad u_x \leq \theta, \quad \text{and} \quad (u_x - \theta)(u - g) = 0. \quad (2.11)$$

These conditions mean that the expansion of the free edge is restricted by the rigid obstacle ( $u \leq g$ ) and the stress, when in contact is compressive ( $\sigma = u_x - \theta \leq 0$ ). Consequently, either there is contact and  $u = g$ , or the edge is free and  $\sigma = 0$ .

Finally, we consider the temperature condition at the free edge. The Dirichlet condition  $\theta = 0$  was used in Gilbert et al. (1990) and Shi and Shillor (1990), since mathematically it was very convenient. However, it was not very realistic, especially when the edge was farther from the obstacle, and the heat exchange or radiation condition  $-\theta_x = \kappa \theta$  was used in Shi and Shillor (1992) with  $\kappa = \text{const}$ . A more realistic assumption is that as the edge approaches the wall there should be an increase in the thermal interaction, and thus  $\kappa$  should depend on the distance of the edge from the wall. When contact is established we may assume either that the contact is perfect, or that there is some residual

<sup>3</sup> In a ‘weak’ sense.

resistance to the flow of heat, which is likely to depend on the contact stress. An idealised case of thermal insulation when there is no contact and perfect thermal contact otherwise, can be represented by

$$\kappa = \begin{cases} 0, & u < g, \\ \infty, & u = g, \end{cases}$$

and was considered in Barber et al. (1980) and in Johnson (1985), among others. It leads to the nonexistence of steady state solutions for a certain range of the parameters  $a$  and  $g$ . However, Duvaut (1980) pointed out that such a condition leads to severe mathematical difficulties in the formulation of the problem. For example, when in contact, the edge has the temperature  $\theta = 0$  which causes the rod to contract instantaneously, and then the edge is insulated so the rod expands and comes into contact, again, leading to infinitely fast oscillations.

#### 2.4. Barber's heat exchange condition

These difficulties with the modelling of the thermal interaction led J. Barber in Barber (1978) to propose what he called the *imperfect thermal condition*, modelling the behaviour of  $\kappa$  when the edge is very close to the obstacle, essentially allowing  $\kappa$  to be a graph, with a vertical segment. Actually, he postulated the following *three* cases:

(i) *Perfect contact* – where

$$\theta = 0 \quad \text{when } u = g \quad \text{and } \sigma < 0.$$

(ii) *Imperfect contact* – where

$$\theta \theta_x < 0 \quad \text{when } u = g \quad \text{and } \sigma = 0.$$

(iii) *No contact* – where

$$\theta_x = 0, \quad \text{when } u < g \quad \text{and } \sigma = 0,$$

and these contact conditions have been used in, e.g., Comninou and Dundurs (1979). In Andrews et al. (1993) a regularised version of Barber's condition (i)-(iii) was studied by introducing the variable

$$r(t) = \sigma(1, t) + (g - u(1, t)), \quad (2.12)$$

which is non-positive when there is contact since  $g = u(1, t)$  and  $r = \sigma \leq 0$ ; when there is no contact  $\sigma(1, t) = 0$  and then  $r = g - u(1, t) > 0$ . Therefore, when  $r$  is positive it is the distance between the rod edge and the obstacle, and when negative  $r$  is the contact stress. Then, instead of the perfect contact assumption (i), it was assumed that the heat transfer coefficient  $\kappa$  was a decreasing function of  $r$ . This assumption was consistent with the existence of a thin layer at the edge that prevents perfect thermal contact, although its resistance decreased with the increase of the (absolute value of the) stress. Also, instead of the non-contact assumption (iii), it was supposed that there was heat exchange and the edge was not insulated. Such assumptions led to the replacement of (iii) by the graph  $\mathcal{K}$ ,

$$\mathcal{K}(r) = \begin{cases} \kappa_1(r) & r < 0 \\ [\kappa_2(0), \kappa_1(0)] & r = 0 \\ \kappa_2(r) & r > 0, \end{cases} \quad (2.13)$$

where  $\kappa_1(r)$  and  $\kappa_2(r)$  are given smooth and decreasing functions such that  $\kappa_2(0) \leq \kappa_1(0)$ . Note the vertical segment  $[\kappa_2(0), \kappa_1(0)]$  is when contact commences and a possible form of  $\mathcal{K}$  is depicted in Fig. 4.

This version of Barber's condition may be written as

$$-\theta_x = \kappa \theta, \quad (2.14)$$

where  $\kappa$  is selected from the graph  $\mathcal{K}$ , i.e.,  $\kappa \in \mathcal{K}$ . Barber's imperfect thermal contact condition, (i)-(iii), can be derived as a limiting case of (2.14) by setting  $\kappa_1(r) \equiv +\infty$ ,  $\kappa_2(r) \equiv 0$  and replacing the segment  $[\kappa_2(0), \kappa_1(0)]$  by the half-line  $[0, \infty)$ . It was found in Andrews et al. (1993) that, when the problem is quasistatic ( $b = 0$ ), then

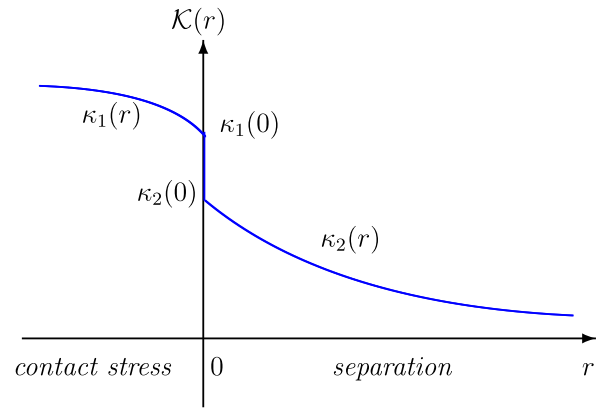


Fig. 4. The heat exchange coefficient multi-function  $\mathcal{K}(r)$ . When  $r > 0$  then  $r = g - u(1, t)$  measures the (dimensionless) gap, and when  $r < 0$ , then  $r = \sigma(1, t)$  measures the (dimensionless) contact pressure. The vertical segment at  $r = 0$  represents the possible values when contact is just established (case (ii)).

the problem with the Barber condition takes a very unusual form mathematically; nonetheless, the existence of the weak solution was established in Andrews et al. (1993).

An experimental attempt to determine the shape of the graph in Fig. 4 was performed in Barber et al. (2003). Away from 0, the shape was found similar to the one in the figure. However, finding experimentally the shape of  $\mathcal{K}$  at 0, i.e., when contact commences, was too difficult. So the question of whether there is a jump at 0 or the graph is continuous is open.

The Barber heat exchange condition (2.14) not only fits well within the theory of variational inequalities and differential set-inclusions, but it has served as an impetus for the further development of MTCM, usually assuming that (2.14) holds point-wise on a curve (in 2D) or on a surface (in 3D).

The main mathematical difficulty in analysing models with Barber's condition lies in the fact that it is associated with mechanical contact conditions, which are intrinsically non-smooth (there is a ceiling on the regularity of the solutions), and it adds another level of complexity to the structure, since the condition is non-smooth, too. To deal with such non-smooth conditions, one resorts to various ways of regularising (smoothing) approximations. Indeed, very often a very small viscosity term is added so the material is assumed to be thermoviscoelastic, which helps with the analysis but causes numerical difficulties. These difficulties often show up in numerical methods for contact problems, with or without thermal effects, as instabilities and non-convergence of the computations, Wriggers (2006). Too often, these are dealt with ad-hoc approaches that do not guarantee the validity of the numerical solutions.

#### 2.5. MEMS actuator

A recent application of Barber's condition in a MEMS setting can be found in Paoli and Shillor (2021). Here, we provide the details of the beam-rod model and mention some of the results. The setting, depicted in Fig. 5, is very common in many MEMS systems, such as switches, grippers, actuators etc., which, in large numbers, can be found in cellphones, TV sets, computers, and other electronic devices.

In this setting, a horizontal beam (vibrating vertically) is rigidly connected at  $(0, 0)$  to a vertical rod (also vertically vibrating), while it is clamped at  $x = L_b$ , both made of silicon. When an electric current flows in the system, the beam may vibrate vertically, while the rod may vibrate vertically because of the beam vibrations, or may expand or contract, as a result of thermal or mechanical forces. The way this MEMS actuator functions is as follows; when an electric current flows in



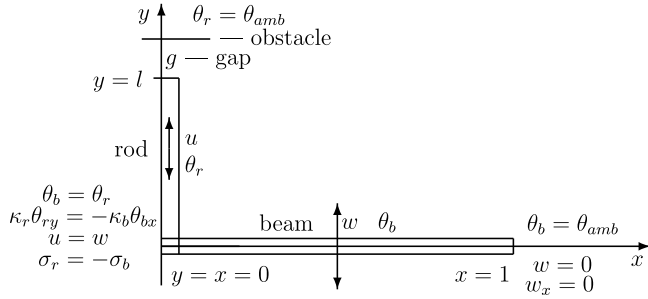


Fig. 5. MEMS actuator (Paoli and Shillor, 2021). The beam (horizontal) is joined to the rod (vertical) at  $x = y = 0$ .

the beam-rod system, the rod expands, comes in contact with the top, the ‘obstacle’ and closes an electric circuit, activating whatever function it controls; once the current stops, the rod cools, contracts and contact is lost.

In a dimensionless model, let  $w(x, t)$  denote the transverse displacement of the beam’s central axis, its temperature be  $\theta_b(x, t)$ , and suppose that it is supported at  $x = 1$  where it has the ambient temperature  $\theta_{amb}$ , scaled to be zero. As a first order approximation, the vibrations and the temperature in the beam are not coupled; see, e.g., Howell et al. (2009). The rod’s vertical displacement is  $u(y, t)$  and its temperature is  $\theta_r(y, t)$ . It is rigidly connected to the beam at  $y = 0$  where the temperature is continuous. Also, the gap (in the reference configuration) between the rod’s top end and the rigid obstacle is  $g$ , and the obstacle is situated at  $y = l + g$ .

The interests lie in the effects of the interaction at  $x = 0 = y$  and the contact process at  $y = l$  on the system dynamics.

The beam’s dynamic vibrations are modelled by

$$w_{tt} + c_b^2 w_{xxxx} + v_b w_{xxxxt} = f_b, \quad (2.15)$$

where  $c_b^2$  is the beam’s scaled elastic modulus,  $v_b \geq 0$  is the scaled viscosity coefficient and  $f_b$  is a (possible) vertical force acting on the beam. The beam temperature satisfies

$$c_{bh} \theta_{bt} - \kappa_b \theta_{bxx} + h_b \theta_b = Q_b(\theta_b), \quad (2.16)$$

where  $c_{bh}$  is the scaled heat capacity;  $\kappa_b$  is the coefficient of heat conduction;  $h_b$  is the coefficient of heat exchange;  $Q_b(\theta_b)$  represents the Joule heating; and the beam exchanges energy with the environment with rate  $h_b \theta_b$ .

The scaled vibrations in the rod are modelled by

$$u_{tt} - c_r^2 u_{yy} - v_r u_{yyt} + \alpha_r \theta_{ry} = f_r, \quad (2.17)$$

where  $c_r^2$  is the scaled elastic modulus of the rod,  $\alpha_r$  is its coefficient of thermal expansion and  $f_r$  is a possible applied vertical force. Also,  $v_r \geq 0$  is the viscosity coefficient. The corresponding energy equation is,

$$c_{rh} \theta_{rt} - \kappa_r \theta_{ryy} + \alpha_r u_{yt} + h_r \theta_r = Q_r(\theta_r), \quad (2.18)$$

where,  $c_{rh}$ ,  $\kappa_r$  and  $h_r$  are the scaled heat capacity, thermal conductivity, and coefficient of heat exchange, respectively, and  $Q_r(\theta_r)$  represents a heat source, which in MEMS actuators is the Joule heating.

We note that the dimensionless shear stresses in the beam and in the rod are given, respectively, by

$$\begin{aligned} \sigma_b(x, t) &= -c_b^2 w_{xxx}(x, t) - v_b w_{xxxx}(x, t), \\ \sigma_r(y, t) &= c_r^2 u_{y}(y, t) + v_r u_{yy}(y, t) - \alpha_r \theta_r(y, t). \end{aligned} \quad (2.19)$$

Crucially, as discussed in Andrews et al. (1993), the Barber heat exchange condition, (2.14) and (2.13), is as follows. First, we let contact variable  $r$  be as above,

$$r(t) = \underbrace{(g - u(l, t))_+}_{\text{distance - no contact}} - \underbrace{(u(l, t) - g)_+}_{\text{penetration}} = g - u(l, t),$$

where

$$(r)_+ = \begin{cases} 0 & r < 0, \\ r & r \geq 0. \end{cases}$$

Thus, when there is no contact  $r = g - u(l, \cdot) > 0$  is the distance of the rod’s top from the obstacle, and when in contact  $r = -(u(l, \cdot) - g)_+ \leq 0$  and it measures the resistance to interpenetration. The heat exchange graph  $\mathcal{K}$  has the form depicted in Fig. 4, and, assuming that the obstacle is kept at the ambient temperature, the heat exchange condition is

$$-\kappa_r \theta_{ry}(l, t) \in \mathcal{K}(r) \theta_r(l, t). \quad (2.20)$$

The mathematical model for the dynamics of the system with a regularised Signorini condition, is as follows.

**Model 2.1.** Find the displacement fields  $w = w(x, t)$ ,  $u = u(y, t)$ , and the temperature fields  $\theta_b = \theta_b(x, t)$ ,  $\theta_r = \theta_r(y, t)$ , for  $x \in [0, 1]$ ,  $y \in [0, l]$  and  $t \in [0, T]$ , such that (2.15)–(2.18) hold for  $t \in (0, T)$ , together with: the boundary conditions:

$$\begin{aligned} w(1, t) &= w_x(1, t) = 0, \quad \theta_b(1, t) = 0, \\ w(0, t) &= u(0, t), \quad \sigma_b(0, t) = -\sigma_r(0, t), \quad w_x(0, t) = 0, \\ \theta_b(0, t) &= \theta_r(0, t), \quad \kappa_b \theta_{bx}(0, t) = -\kappa_r \theta_{ry}(0, t); \end{aligned}$$

the contact conditions:

$$\begin{aligned} \sigma_r(l, t) &= -c_n [(u(l, t) - g)_+], \\ -\kappa_{rth} \theta_{ry}(l, t) &= h(t) \theta_r(l, t), \end{aligned}$$

where  $r(t) = g - u(l, t)$  and

$$h(t) \in \mathcal{K}(r(t));$$

the initial conditions:

$$w(x, 0) = w_0(x), \quad w_t(x, 0) = w_{0v}(x), \quad (2.21)$$

$$u(y, 0) = u_0(y), \quad u_t(y, 0) = u_{0v}(y), \quad (2.22)$$

$$\theta_b(x, 0) = \theta_{b0}(x), \quad \theta_r(y, 0) = \theta_{r0}(y); \quad (2.23)$$

the initial displacements  $w_0(x)$ ,  $u_0(y)$ , velocities  $w_{0v}(x)$  and  $u_{0v}(y)$ , and temperatures  $\theta_{b0}(x)$  and  $\theta_{r0}(y)$  are prescribed functions.

It was established in Paoli and Shillor (2021) that the problem has a weak solution, assuming that the input functions are smooth. This was accomplished by using a Galerkin method, which in addition to its theoretical aspects, is also easy to implement in FEM algorithms. The uniqueness of the solutions remains an unresolved question.

We conclude that the Barber heat exchange condition has become an integral part of MTCM, leading to the expansion of the theory. However, there exist open issues that need to be addressed to have a more complete understanding of its mathematical structure and its many applications. The main one is the construction of effective algorithms for problems with contact and heat exchange, with guaranteed convergence of the simulations to the solutions. In particular, there is a need to find effective ways to regularise both the contact conditions and the Barber condition for numerical simulations, while retaining the physical acceptability. Mathematically, there is considerable interest in studying the ways contact may be established and lost.

### 3. Thermoelastic contact with wear

#### 3.1. Barber’s experiment

We now turn to thermoelastic models that incorporate the effects of friction and wear. Barber’s celebrated 1969 experiment (Barber, 1969) involved a set of 3 thermoelastic rods fixed to a base and pressed against a surface that moves tangentially at speed  $V$ , as illustrated in Fig. 6 with  $N = 2$ . The sliding contact with the rods introduces two new elements to the model; the first one is frictional heating, at a

rate proportional to the compressive stress between each rod and the moving surface. Assuming that the surface is maintained at a constant ambient temperature  $\theta_0$ , we write the heat transfer condition at the boundary of the  $i$ th rod in the form

$$k\theta_{ix} = \frac{\theta_0 - \theta_i}{R_i} - fV\sigma_i \quad \text{at } x = 1, \quad (3.1)$$

where  $R_i$  is the ‘contact resistance’ and  $f$  is the coefficient of friction.

The second new feature to be modelled is frictional wear. Inspired by Barber (1969), a model that assesses the relative importance of wear and thermoelasticity for the 2-rod problem was proposed in Ockendon and Barber (2016). According to Archard’s law (Archard, 1953), material is removed from the end of the rod at a rate proportional to the frictional energy dissipation rate. The dimensional length of the  $i$ th rod may thus be expressed as  $\ell_i(t) = L + u_i(1, t) - w_i(t)$ , where the rate of wear is modelled as

$$w'_i(t) = -\beta fV\sigma_i(1, t), \quad (3.2)$$

and  $\beta$  is a constant of proportionality.

We non-dimensionalise the problem as in (2.7), so that the dimensionless temperature  $\theta_i(x, t)$  and displacement  $u_i(x, t)$  satisfy Eqs. (2.8). As suggested in Section 2.3, we take the quasistatic limit where the two parameters  $a^2$  and  $b$  are negligible, so that the system for the  $i$ th rod reduces to

$$\theta_{it} - \theta_{ixx} = 0, \quad (3.3a)$$

$$u_{ix} - \theta_i = \sigma_i(t), \quad (3.3b)$$

where the stress  $\sigma_i$  is spatially uniform. The total stress summed over all of the rods is determined by the applied compressive stress  $F$ , which is assumed to be a specified constant. By choosing

$$\Delta\theta = \frac{F}{(3\lambda + 2\mu)\alpha} \quad (3.4)$$

in (2.7), we can thus take

$$\sum_i \sigma_i(t) = -1. \quad (3.5)$$

We assume Newton cooling at the base, so that

$$\theta_{ix} = h\theta_i \quad \text{at } x = 0, \quad (3.6)$$

where  $h$  is a dimensionless heat transfer coefficient. At the other end of each rod, we impose the dimensionless versions of the conditions stated above. The heat transfer condition (3.1) becomes

$$\theta_{ix} + \kappa_i\theta_i = -\gamma\sigma_i \quad \text{at } x = 1, \quad (3.7)$$

and the dimensionless perturbation to the length of the  $i$ th rod is given by

$$d_i(t) = u_i(1, t) - w_i(t) = \sigma_i(t) + \int_0^1 \theta_i(x, t) dx - w_i(t), \quad (3.8a)$$

where

$$w'_i(t) = -\eta\sigma_i(t). \quad (3.8b)$$

The new dimensionless parameters are given by

$$\gamma = \frac{fV(3\lambda + 2\mu)\alpha L}{k}, \quad \kappa_i = \frac{L}{kR_i}, \quad \eta = \frac{\beta fF(\lambda + 2\mu)\rho c L}{k}. \quad (3.9)$$

The problem is closed by the Signorini contact condition (2.11). Here the gap between the  $i$ th rod and the moving surface is determined by the longest rod (or rods) and given by  $d - d_i$ , where  $d = \max_j d_j$ , so our version of (2.11) reads

$$d_i \leq d, \quad \sigma_i \leq 0, \quad \sigma_i(d_i - d) = 0 \quad \text{for all } i. \quad (3.10)$$

Note that this condition determines  $d$ : by (3.5), at least one  $\sigma_i$  must be nonzero and therefore  $d_i$  must equal  $d$  for some  $i$ .

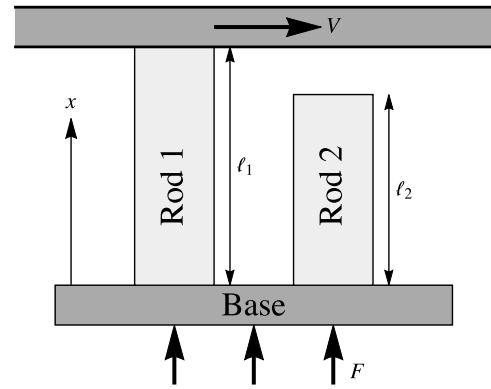


Fig. 6. Schematic of two thermoelastic rods pressed with a force  $F$  against a surface moving at speed  $V$ .

As in Section 2.4, we define a variable  $r$  which combines the stress in the rod with the gap between the rod and the obstacle. In the present case, the equivalent definition to (2.12) for rod  $i$  is

$$r_i(t) = \sigma_i(t) + d(t) - d_i(t). \quad (3.11)$$

Thus  $r_i$  is negative when the  $i$ th rod is in contact with the moving surface, positive when it is out of contact, and zero when it is transitioning between these two states. Recall from Section 2.4 that Barber’s heat exchange condition poses a (generalised) functional relation between the dimensionless heat-transfer coefficient  $\kappa_i$  and  $r_i$ . Moreover, we can easily express  $\sigma_i$  as a function of  $r_i$ , namely

$$\sigma_i = (r_i)_- = \begin{cases} r_i & r_i < 0, \\ 0 & r_i \geq 0. \end{cases} \quad (3.12)$$

We can therefore eliminate  $u_i$  and  $\sigma_i$  from the problem. The temperature in rod  $i$  satisfies the heat equation (3.3a) and the standard Robin boundary condition (3.6) at  $x = 0$ . The heat transfer condition (3.7) at the top of the rod takes the form

$$\theta_{ix} + \kappa_i\theta_i = -\gamma(r_i)_- \quad \text{at } x = 1, \quad (3.13)$$

and by differentiating (3.8a) with respect to  $t$  we express the wear equation as

$$r'_i(t) = d'(t) + (\gamma - \eta)(r_i)_-(t) + h\theta_i(0, t) + \kappa_i\theta_i(1, t). \quad (3.14)$$

The remaining unknown  $d'(t)$  is in principle determined by the constraint (3.5), i.e.

$$\sum_i (r_i)_-(t) = -1. \quad (3.15)$$

As noted in Section 2.4, the precise form of the relation between  $\kappa_i$  and  $r_i$  may be difficult to determine. We henceforth make the simplifying assumption that the dimensionless heat transfer coefficients  $\kappa_i$  defined by (3.9) are all negligible, i.e. that the surface sliding past the rods is a relatively poor thermal conductor, even when in contact. In this limit, the problem (3.3a), (3.6), (3.13) for the temperature in each rod is simplified to

$$\theta_{it} - \theta_{ixx} = 0, \quad 0 < x < 1, \quad (3.16a)$$

$$\theta_{ix} = h\theta_i \quad x = 0, \quad (3.16b)$$

$$\theta_{ix} = -\gamma(r_i)_- \quad x = 1. \quad (3.16c)$$

Since the system (3.16) is now linear, given an appropriate initial condition we can in principle determine the temperature  $\theta_i(x, t)$  as a linear functional of the normalised heating  $-\gamma(r_i)_-(t)$  applied at  $x = 1$ . In particular, we can express the heat flux at  $x = 0$  in the form

$$\theta_{ix}(0, t) = -\gamma Q[(r_i)_-](t) := -\gamma \int_0^t (r_i)_-(\tau) G(h; t - \tau) d\tau, \quad (3.17)$$

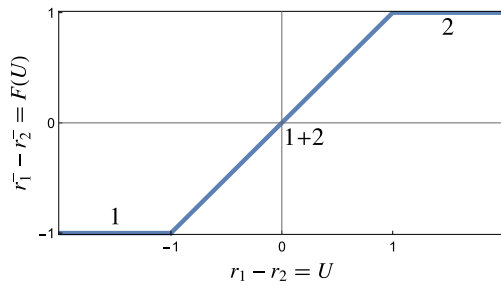


Fig. 7. The function  $F(U)$  defined by (3.22). The annotations indicate the regions where (1) pin 1, (2) pin 2, (1+2) both pins are in contact.

where  $G$  denotes the relevant Green's function (which depends parametrically on  $h$ ; see Howell et al., 2018; Howell, 2018 for details). For future reference, we note that the Laplace transform of  $G$  is given by

$$\bar{G}(h; p) = \left[ \cosh(\sqrt{p}) + \frac{\sqrt{p}}{h} \sinh(\sqrt{p}) \right]^{-1}. \quad (3.18)$$

We can use (3.17) to eliminate the temperature from the problem and express (3.14) as an integro-differential-algebraic system of the form

$$r'_i = d' + (\gamma - \eta)(r_i)_- - \gamma Q[(r_i)_-] \quad (3.19)$$

where, as above, the constraint (3.15) in principle determines the additional unknown  $d'(t)$ .

We can also exploit the linearity to sum over  $i$  and find that, after neglecting transients,

$$d(t) = \bar{r}(t) + \frac{\gamma t}{N}, \quad (3.20)$$

where  $\bar{r}$  is the average of the quantities  $r_i$  over all the rods. The net conservation Eqs. (3.15) and (3.20) allow us to effectively eliminate one of the rods and project the  $N$ -rod problem onto  $(N-1)$  dimensions, as we will illustrate below for the cases  $N=2$  and  $N=3$ .

### 3.2. The two-pin problem

When there are just two pins, we can subtract the instances of (3.19) with  $i=1$  and  $i=2$  to obtain a problem that depends only on  $U(t) := r_1(t) - r_2(t)$ . The only challenge is to express  $(r_1)_- - (r_2)_-$  as a function of  $U$ . From the constraint (3.15), namely

$$(r_1)_- + (r_2)_- = -1 \quad (3.21)$$

in this case, we see that there are three possibilities to consider. If both  $r_1$  and  $r_2$  are negative, then both of the rods are in contact, but if  $r_2 \geq 0$  then only pin 1 is in contact and  $r_1 = -1$ , and *vice versa*. By considering each of these cases in turn, one easily finds that  $(r_1)_- - (r_2)_- = F(U)$ , where the function  $F$  is given by

$$F(U) = \frac{1}{2}(|U+1| - |U-1|) \quad (3.22)$$

and plotted in Fig. 7. The problem thus boils down to the nonlinear integro-differential equation

$$U' = (\gamma - \eta)F(U) - \gamma Q[F(U)]. \quad (3.23)$$

Eq. (3.23) admits the trivial steady solution  $U=0$ , corresponding to both of the pins being in contact and sharing the applied load equally, so that  $r_1 = r_2 = -1/2$ . Since  $F(U) = U$  for  $|U| < 1$ , the linearised version of (3.23), namely

$$U' = (\gamma - \eta)U - \gamma Q[U], \quad (3.24)$$

holds without approximation as long as  $|U| < 1$ . It follows that perturbations to the trivial solution must either decay or grow exponentially until  $|U| = 1$ , i.e. it is impossible for the solution to saturate at a finite amplitude with  $0 < |U| < 1$ .

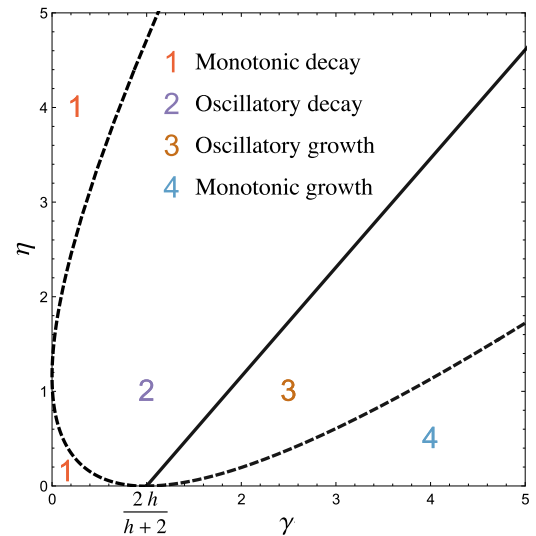


Fig. 8. The  $(\gamma, \eta)$  parameter space plotted with  $h=2$ . The solid curve delineates regions where the trivial solution is linearly stable or unstable, while the dashed curve delineates regions where the behaviour is monotonic or oscillatory.

The linear growth rates  $\lambda$  satisfy

$$\lambda + \eta - \gamma + \gamma \bar{G}(h; \lambda) = 0, \quad (3.25)$$

where  $\bar{G}$  is defined by (3.18). For given values of the parameters  $\{\gamma, \eta, h\}$ , the stability of the system depends on whether (3.25) admits any roots  $\lambda$  with positive real part. Furthermore, whether the resulting exponential growth or decay is monotonic or oscillatory depends on whether  $\lambda$  is real or complex. As shown in Fig. 8, the  $(\gamma, \eta)$  parameter space can be divided into four regions: in regions 1 and 2 the trivial solution is stable, while in regions 3 and 4 it is unstable. The figure here is plotted with  $h=2$ , but the overall structure is unchanged for other values of  $h$ . Generally we see that increasing  $\gamma$  destabilises the system, while increasing  $\eta$  stabilises it. Looking back at the definitions (3.9), we recall that  $\gamma$  and  $\eta$  measure the effects of frictional heating and wear, respectively.

The predictions of the stability analysis can be tested by solving the problem (3.23) numerically for parameter values lying in each of the regions labelled 1–4 in Fig. 8. Typical solutions are shown in Fig. 9, where we fix  $h=2$  and  $\eta=0.2$  while varying  $\gamma$ , with the initial condition  $U(0)=0.2$  in each case. As  $\gamma$  increases, we move sequentially through the cases of monotonic decay, oscillatory decay, oscillatory growth and monotonic growth. As predicted, the behaviour is purely exponential for  $|U| < 1$ , and the nonlinearity becomes evident only when  $|U|$  is larger than 1. With  $\gamma=2$  the system undergoes large-amplitude nonlinear oscillations, in which  $|U|$  is usually greater than 1. The physical interpretation is that, for most of the time, only one of the two pins is in contact, and the transfers of the load between the two pins (i.e. when  $|U| < 1$ ) occur very rapidly. These effects become ever more pronounced as  $\gamma$  increases further, leading to extremely violent oscillations that could be associated with unpleasant phenomena such as brake and clutch judder.

This behaviour is explained and quantified in Howell (2018) by asymptotic analysis of Eq. (3.23) in the limit  $\gamma \rightarrow \infty$ . If  $\gamma \gg \eta$  then the effects of wear are negligible, and the system always undergoes violent oscillations. If  $\eta \gg \gamma \gg 1$  then the effects of wear are dominant, and the system always converges to the trivial steady solution  $U=0$ . The transition between these two limiting states occurs when  $\eta/\gamma = O(1)$ , and is summarised in Fig. 10.

For fixed  $h > 0$ , if we start at the top of the diagram with  $\eta/\gamma \gtrsim 1.12$ , then only the trivial solution  $U=0$  is stable. Now decreasing  $\eta$  or increasing  $\gamma$ , i.e. increasing the importance of frictional heating relative

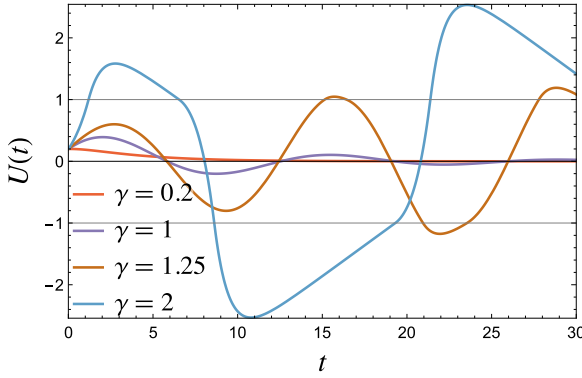


Fig. 9. Numerical solutions  $U(t)$  of Eq. (3.23) subject to  $U(0) = 0.2$  with parameter values  $h = 2$ ,  $\eta = 0.2$  and  $\alpha \in \{0.2, 1, 1.25, 2\}$ .

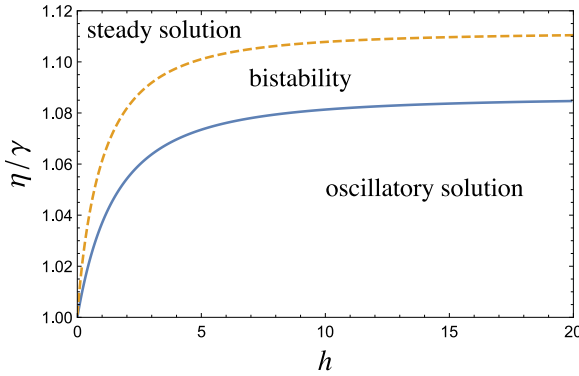


Fig. 10. The  $\eta/\gamma$  versus  $h$  parameter space obtained in the limit  $\gamma \rightarrow \infty$ .

to wear, we move downwards through the parameter space. The trivial solution remains stable until we reach the lower blue solid curve, at which point it loses stability (this stability boundary corresponds to the solid curve in Fig. 8). As soon as we cross this curve, the system evolves into a periodic solution in which  $U(t)$  undergoes large nonlinear oscillations with amplitude of order  $\gamma \gg 1$ . If we now increase  $\eta/\gamma$  again, the oscillatory solution persists until we cross the upper orange dashed curve, at which point it suddenly switches off and the system reverts to the steady state  $U = 0$ . Between the two curves, the system is bistable, and can either reach a steady state or perform violent oscillations depending on the initial conditions.

### 3.3. The three-pin problem

For the case of  $N = 3$  pins, the problem can be projected onto  $N - 1 = 2$  dimensions by taking linear combinations of the three governing equations (3.23) (with  $i = 1, 2, 3$ ) and using the constraint (3.15). Here we choose to define the three variables

$$U_1 = r_1 - r_2, \quad U_2 = r_3 - r_1, \quad U_3 = r_2 - r_3,$$

so that  $\mathbf{U} = (U_1, U_2, U_3)^T$  lives on the plane  $U_1 + U_2 + U_3 = 0$ . The governing equation for  $\mathbf{U}$  reads

$$\mathbf{U}' = (\gamma - \eta)\mathbf{F}(\mathbf{U}) - \gamma\mathbf{Q}[\mathbf{F}(\mathbf{U})], \quad (3.26)$$

where we denote

$$\begin{pmatrix} (r_1)_- - (r_2)_- \\ (r_3)_- - (r_1)_- \\ (r_2)_- - (r_3)_- \end{pmatrix} = \mathbf{F}(\mathbf{U}), \quad (3.27)$$

and we recall that  $(r_j)_-$  have to satisfy the constraint (3.15), i.e.

$$(r_1)_- + (r_2)_- + (r_3)_- = -1. \quad (3.28)$$

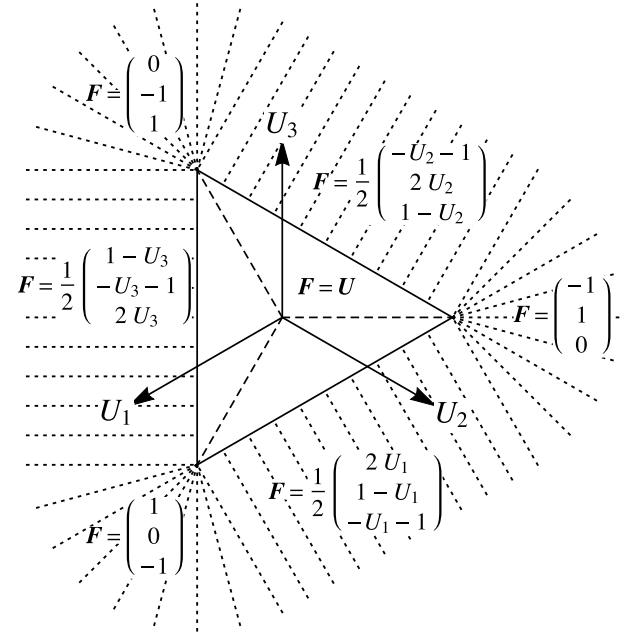


Fig. 11. The function  $\mathbf{F}(\mathbf{U})$  defined by Eq. (3.27), evaluated on the plane  $U_1 + U_2 + U_3 = 1$ .

As in Section 3.2, the function  $\mathbf{F}$  may be evaluated by dividing up the solution space according to whether each pin is in or out of contact. The result is depicted in Fig. 11. Inside the central equilateral triangle, all three pins are in contact, so  $(r_j)_- < 0$  for all  $j$  and  $\mathbf{F}(\mathbf{U}) = \mathbf{U}$ . In the regions swept out by rays normal to the edges of the triangle, just two pins are in contact. For example, in the region just below the  $U_2$  axis, pins 1 and 2 only are in contact, so that  $(r_1)_- < 0$ ,  $(r_2)_- < 0$  and  $(r_3)_- = 0$ . With this information and the constraint (3.28), in this region we can express  $\mathbf{F}(\mathbf{U})$  just in terms of  $U_1$ , as shown in the figure. In the remaining regions swept out by rays radiating from the vertices of the triangle, just one pin is in contact. For example, in the rightmost such region in Fig. 11, only pin 1 is in contact, so  $(r_1)_- = -1$  and  $(r_2)_- = (r_3)_- = 0$ .

Having defined the function  $\mathbf{F}$ , we can now go ahead and solve Eq. (3.26) numerically. Some typical results are shown in Fig. 12, where we fix  $h = 2$  and  $\eta = 2.5$  while varying  $\gamma$ . The annotations indicate regions where each pin is in or out of contact, which are demarcated by the straight lines. Recall that all three pins are in contact inside the central equilateral triangle.

In Fig. 12(a), we set  $\gamma = 0.2$ , which is within the region marked 1 in Fig. 8 so, as expected, the solution decays monotonically to the trivial steady state. Fig. 12(b) shows the behaviour with  $\gamma = 2.5$ , which is in region 2, and the solution indeed displays a stable spiral behaviour as  $\mathbf{U} \rightarrow \mathbf{0}$ .

Next consider Fig. 12(d), where  $\gamma = 10$  so the zero solution is subject to a monotonic instability. With this large value of  $\alpha$ , the solution undergoes large-amplitude nonlinear oscillations with amplitude of order  $\gamma$ , consistently with the results of the two-pin problem in Section 3.2. The system spends most of the time with just one pin in contact, with very sudden switches occurring as the load transitions from one pin to another. Finally, Fig. 12(c) shows the intermediate case  $\gamma = 4$ , where the origin is predicted to be an unstable spiral. In this case, the solution indeed grows until it exits the central region where all three pins are in contact, but then appears to lack the energy to completely escape its influence. Instead, the system undergoes apparently chaotic oscillations, where it spends significant time with either one, two, or three pins in contact.



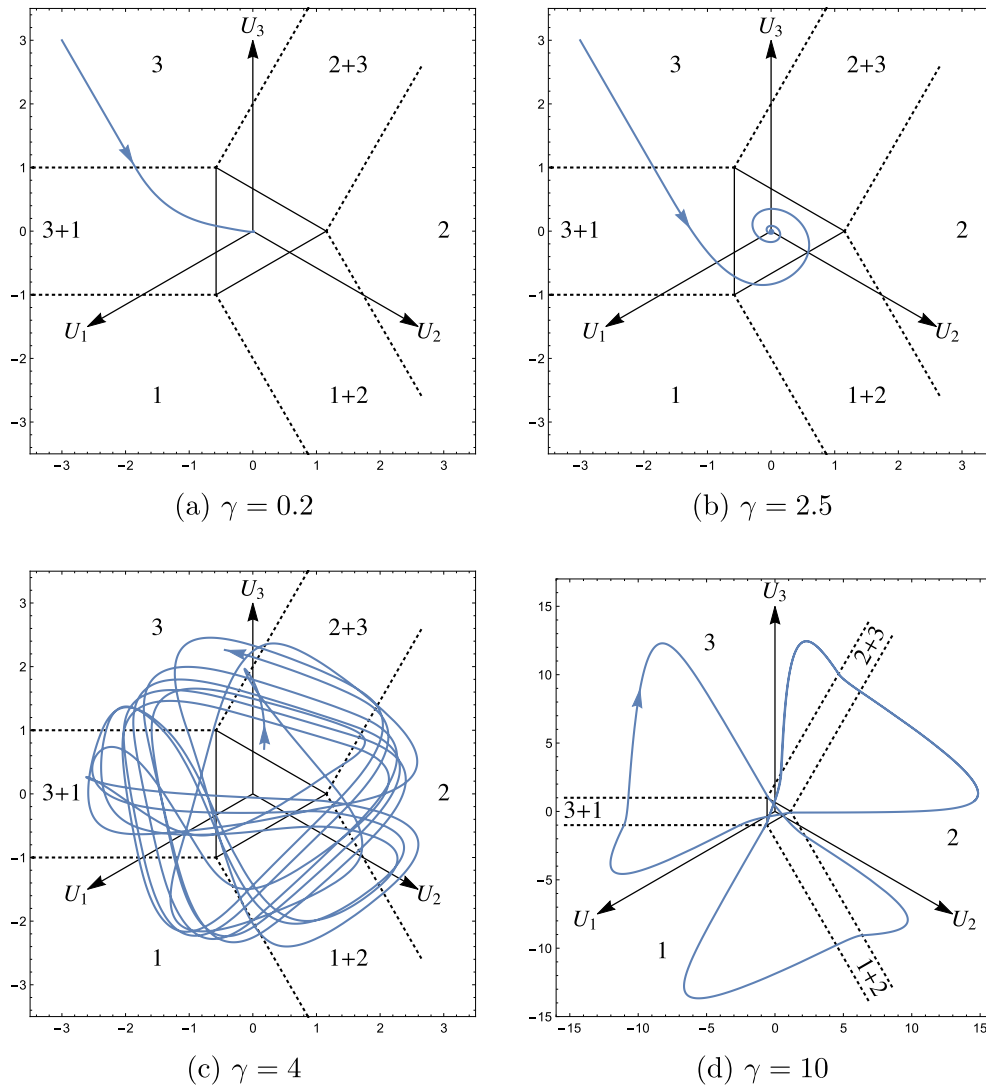


Fig. 12. Numerical solutions of the 3-pin problem (3.26) with  $h = 2$ ,  $\eta = 2.5$  and  $\gamma \in \{0.2, 2.5, 4, 10\}$ .

#### 4. Discussion

We have described two classes of dynamic thermoelastic problems to illustrate how modelling pioneered by Jim Barber has led to substantial new areas of mathematical research. Hopefully, this research has improved our understanding of phenomena ranging from the operation of MEMS devices to the sliding of brake blocks.

The first class of models considers general one-dimensional ‘rod-contact’ problems in the absence of wear under the assumption of Barber’s ‘imperfect’ contact conditions. These conditions model the complicated switching behaviour that can occur when contact is made or lost. This has opened up a novel area of research into the mathematical theory of free boundary problems in which the free boundary configuration can be difficult to determine. In general, the resulting models can only be solved numerically, and much work remains to be done to validate the relevant discretisations. However, the ‘weak solution’ theories that have emerged have been able to provide the required mathematical underpinning in realistic situations.

In the second class of multi-rod models in which wear effects may be comparable to thermoelastic effects, the further development of Barber’s pioneering experimental and theoretical research has benefited from the application of modern asymptotic analysis and the theory of dynamical systems. This has revealed a multitude of modes in which the contact switches from rod to rod. In simple cases results have been

obtained in accord with Barber’s experiments. However, it is now clear that even with 2 or 3 rods the switching of contact from rod to rod can become more and more violent as the friction coefficient increases in comparison with the wear coefficient. Hence, it would be of interest to generalise Barber’s experiments in order to compare rods of different roughness.

The authors are very happy to be part of this celebration of Jim Barber’s birthday and we wish him many more years of fruitful research.

#### Declaration of competing interest

The authors declare that they have no known competing financial interests or personal relationships that could have appeared to influence the work reported in this paper.

#### References

- Ahn, J., Kuttler, K.L., Shillor, M., 2017. Modeling, analysis and simulations of a dynamic thermoviscoelastic rod-beam system. *Differ. Equ. Dyn. Syst.* 25 (4), 527–552.
- Andrews, K.T., Shi, P., Shillor, M., Wright, S., 1993. Thermoelastic contact with Barber’s heat exchange condition. *Appl. Math. Optim.* 28 (1), 11–48.
- Archard, J.F., 1953. Contact and rubbing of flat surfaces. *J. Appl. Phys.* 24 (8), 981–988.
- Barber, J.R., 1969. Thermoelastic instabilities in the sliding of conforming solids. *Proc. R. Soc. A* 312 (1510), 381–394.
- Barber, J.R., 1978. Contact problems involving a cooled punch. *J. Elasticity* 8 (4–5), 409–423.

- Barber, J.R., Dundurs, J., Comninou, M., 1980. Stability considerations in thermoelastic contact. *J. Appl. Mech.* 47 (4–5), 871–874.
- Barber, G.C., Jordan-Steen, M., Shillor, M., 2003. The heat exchange coefficient in thermoelastic contact. *J. STLE* 28 (3), 10–16.
- Bartos, K., Janiczko, T., Szafraniec, P., Shillor, M., 2018. Dynamic thermoviscoelastic thermistor problem with contact and nonmonotone friction. *Appl. Anal.* 97 (8), 1432–1453.
- Bień, M., 2003. Existence of global weak solutions for coupled thermoelasticity with Barber's heat exchange condition. *J. Appl. Anal.* 9 (2), 163–185.
- Carlson, D.E., 1973. Linear thermoelasticity. In: *Linear Theories of Elasticity and Thermoelasticity*. Springer, pp. 297–345.
- Comninou, M., Dundurs, J., 1979. On the Barber boundary conditions for thermoelastic contact. *J. Appl. Mech.* 46, 849–853.
- Duvaut, G., 1980. Equilibre d'un solution elastique avec contact unilatéral et frottement de Coulomb. *C. R. Acad. Sci. Paris* 290 (5), 263–266.
- Duvaut, G., Lions, J.L., 1976. *Inequalities in Mechanics and Physics*. Springer.
- Fichera, G., 1972. Boundary value problems in elasticity with unilateral constraints. In: *Handbuch der Physik VI a/2*. Springer, Berlin, pp. 391–424.
- Gasiński, L., Ochal, A., Shillor, M., 2016. Quasistatic thermoviscoelastic problem with normal compliance, multivalued friction and wear diffusion. *Nonlinear Anal. RWA* 27, 183–202.
- Gilbert, R.P., Shi, P., Shillor, M., 1990. A quasistatic contact problem in linear thermoelasticity. *Rend. Mat. Ser. VII* 10, 785–808.
- Howell, P.D., 2018. Asymptotic analysis of a dynamical system arising in thermoelastic contact. *SIAM J. Appl. Math.* 78 (6), 3145–3167.
- Howell, P.D., Barber, J.R., Ockendon, J.R., 2018. Multiple-contact thermoelastic oscillations. *J. Therm. Stresses* 41 (10–12), 1329–1345.
- Howell, P., Kozyreff, G., Ockendon, J., 2009. *Applied Solid Mechanics*. In: *Cambridge Texts in Applied Mathematics*, Cambridge University Press.
- Johnson, K.L., 1985. *Contact Mechanics*. Cambridge University Press.
- Kikuchi, N., Oden, J.T., 1988. *Contact Problems in Elasticity: A Study of Variational Inequalities and Finite Element Methods*. SIAM, Philadelphia.
- Migórski, S., Ochal, A., Shillor, M., Sofonea, M., 2018. Nonsmooth dynamic frictional contact of a thermoviscoelastic body. *Appl. Anal.* 97 (8), 1228–1245.
- Ockendon, J.R., Barber, J.R., 2016. A model for thermoelastic contact oscillations. *IMA J. Appl. Math.* 81 (4), 679–687.
- Paoli, L., Shillor, M., 2021. A dynamic thermo-mechanical actuator system with contact and barber's heat exchange boundary conditions. *Proc. Roy. Soc. Edinburgh Sect. A* 151 (2), 734–760.
- Shi, P., Shillor, M., 1990. Uniqueness and stability of the solution to a thermoelastic contact problem. *Eur. J. Appl. Math.* 1, 371–387.
- Shi, P., Shillor, M., 1992. Existence of a solution to the  $N$  dimensional problem of thermoelastic contact. *Comm. Partial Differential Equations* 17 (9–10), 1597–1618.
- Shillor, M., 2013. Thermoelastic contact, rod models. In: Hetnarski, R. (Ed.), *Encyclopedia of Thermal Stresses*, Vol. 655. Springer Science & Business Media, Dordrecht.
- Shillor, M., 2020. Models of dynamic contact of a 2D thermoelastic bar. *J. Theoret. Appl. Mech.* 58.
- Shillor, M., Sofonea, M., Telega, J.J., 2004. *Models and Analysis of Quasistatic Contact: Variational Methods*, Vol. 655. Springer Science & Business Media.
- Sofonea, M., Han, W., Shillor, M., 2006. Analysis and Approximations of Contact Problems with Adhesion or Damage. In: *Pure and Applied Mathematics*, vol. 276, Chapman & Hall/CRC Press.
- Wriggers, P., 2006. *Computational Contact Mechanics*. Springer.
- Xu, X., 1996. The  $N$ -dimensional quasistatic problem of thermoelastic contact with Barber's heat exchange conditions. *Adv. Math. Sci. Appl.* 6, 559–587.